Acta of Bioengineering and Biomechanics
Vol. 26, No. 2, 2024

Original paper
DOI: 10.37190/ABB-02433-2024-04

Usefulness of subtraction thermography in the evaluation of blood vessels and lymphatic vessels in the dental pulp

KAMILA WIŚNIEWSKA[1]*, MARIA SZYMONOWICZ[2], PIOTR KUROPKA[3], ZBIGNIEW RYBAK[2], NATALIA STRUZIK[4], KRZYSZTOF D. DUDEK[5], ANNA NIKODEM[6], MACIEJ DOBRZYŃSKI[4]

[1] Department of Dental Surgery, Wroclaw Medical University, Wrocław, Poland.
[2] Pre-Clinical Research Centre, Wroclaw Medical University, Wrocław, Poland.
[3] Department of Histology and Embryology, Wroclaw University of Environmental and Life Sciences, Wrocław, Poland.
[4] Department of Pediatric Dentistry and Preclinical Dentistry, Wroclaw Medical University, Wrocław, Poland.
[5] Department of Logistics and Transport Systems, Faculty of Mechanical Engineering, Wroclaw University of Science and Technology, Wrocław, Poland.
[6] Division of Biomedical Engineering and Experimental Mechanics, Wroclaw University of Technology, Wrocław, Poland.

Purpose: Caries or iatrogenic thermal trauma of the teeth have a significant impact on the dental pulp structure connected with stimulation of angiogenesis and lymphangiogenesis. Therefore, the aim of the study was to identify the difference in the rate of heat dissipation by vessels present in the dental pulp. *Methods*: Freshly extracted healthy (n = 10) and carious (n = 14) molars and premolars were cut on a diamond saw and subjected to active thermographic examination and then subjected to lymphoscintigraphy and X-ray examination. The tooth samples were heated uniformly to 40 ± 0.5 °C. A thermal imaging camera with a resolution of 640 × 320 pixels was used to record the sequence of thermograms during free cooling. Due to the different volume of teeth and different surface conditions of the examined teeth (color, roughness) and the related different radiation emissivity, the changes in the temperature (ΔT) of the tooth cross-section surface were analyzed using the subtractive method within 120 seconds from the switching off of the thermal impulse (heating). *Results*: Thermographic examination of healthy and cariously changed teeth revealed areas of increased tissue fluid flow combined with heat release, which may indirectly indicate the existence of vessels in these areas. On a thermal imaging camera, variations in the rate of heating or cooling across several cross-sectional sections of the same tooth indicate changes in the dental structure's density. *Conclusions*: In caries-affected teeth, intracanalicular fluid flows are different than those of healthy teeth. Therefore, it can be concluded that the pulp vessels enabling circulation of body fluids – blood and lymphatic – increases with the intensity of inflammation. Maintaining the homeostasis of the dental pulp depends heavily on the circulation of bodily fluids within the dental organ.

Key words: *thermography, human dental pulp, lymphatic and blood markers, lymphatic vessels*

1. Introduction

Thermography is a nonionizing, non-invasive, quantitative method for diagnosing periapical inflammatory lesion [1] therefore it is an alternative optical method for detecting lesions in hard and soft tissues of the tooth. This method involves energy conversion using thermal infrared radiation (Planck) from teeth to detect various lesions. This refers to lesions in the enamel and dentin and the associated accelerated demineralization or hypermineralization of collagen and enamel prisms. Moreover, with this technique it is possible to analyze soft tissue fluid flow. Thermophotonic lock-in imaging (TPLI) uses diffusive thermal waves as markers to collect information on the subsurface properties of tooth structure. In this process, a low-power, continuous light source of modulated intensity (e.g., a laser) is used for generating a thermal wave field inside the tooth, followed by infrared emission of the thermal-wave

* Corresponding author: Kamila Wiśniewska, Department of Dental Surgery, Wroclaw Medical University, Wrocław, Poland. E-mail: kamila.wisniewska@umw.edu.pl
Received: April 8th, 2024
Accepted for publication: August 16th, 2024

field. This means that the local change in surface temperature is assessed and averaged over a series of cycles, while heat is periodically introduced into the sample at a specified blocking frequency. The received signal that carries information on sub-surface heterogeneity is assessed. Demodulation of the thermophotonic signal allows phase and amplitude images to be determined from a reference signal (i.e., optical excitation modulation signal) [1].

Important in imaging related to medicine are heat exchange processes occurring in tissues, such as conduction or convection. Basis of the application of thermal imaging in biology and medicine lies in the exchange of heat between the living organism and the environment, which occurs through the surface tissues of the body. The occurrence of changes in the thermal map of the imaged surface of the organism is closely related to the changes that occur in the metabolism and blood supply of internal tissues [12], [38]. Metabolic processes are considered to be the primary source of thermal energy in the body. According to the available literature, nearly 60% of total energy is utilized for the generation of heat [23], [25].

The main cause of inflammation in teeth is dental caries. It is caused by a bacterial agent resulting in demineralisation and subsequent decay of the hard tissues of the tooth. After overcoming the enamel barrier, the caries reaches the dentin, the structure of which is characterised by dentinal tubules. In their lumen, there are odontoblast protuberances, nerve fibres and tissue fluid, which form a living connection between the dentin and the pulp. When the carious process reaches these structures, the pulp's defence reactions are activated. Inflammation is the primary defence mechanism of any vascularised tissue. It is no different in the pulp, where we can distinguish between acute inflammation caused by a saline stimulus or chronic inflammation caused by a milder but long-lasting stimulus. In addition to caries, pulpitis can be caused by traumatic, thermal, chemical and osmotic factors [37].

As a result of damage to the enamel and dentin surfaces by a deep carious lesion or fracture of the tooth tissues due to trauma, bacterial colonisation of the root canals can occur, forming a biofilm that infects the tooth pulp [5], [29]. Very often, bacteria colonise in spaces beyond the reach of dental instruments and antimicrobial agents. Proteins from the remaining necrotic tissue and bacterial adhesives provide nutrients for their survival [6]. The main route of passage of bacterial transformation products (such as lactic acid, propionic acid and acetic acid) in deep caries is through dentinal tubules, which open on contact with acids. At the low pH caused by the presence of the aforementioned acids, a specific by-product released extracellularly by acid-forming Gram-positive bacteria, lipoteicholic acid (LTA), is activated [19], [48].

Odontoblasts express toll-like receptors (*tolls*), which recognise specific pathogens and trigger the recruitment of other immune cells such as dendritic cells and lymphocytes [8], [11]. Other molecules, including beta-defensin [39] or transforming growth factor beta (TGF-b), are also released by odontoblasts. Beta-defensin has a bactericidal effect on bacteria commonly found in caries, such as *Streptococcus mutans and Lactobacillus sp* [34]. TGF-b controls homeostasis, exerting a pro-inflammatory effect in the early phase of injury and an anti-inflammatory and tissue-suppressive effect in the late phase [34], [41].

Because thermography primarily images changes in the infrared radiation intensity of an object and consequently changes in its temperature, it is an excellent tool for imaging inflammation developing in the body. The thermographic measurement method is based on the physical phenomenon that objects with a temperature above absolute zero (0.0 K or –273.15 °C) emit electromagnetic radiation. If its intensity can be determined, the temperature of the emitting object can be calculated without contact. One of the processes accompanying the inflammatory process is an increase in temperature at the site of infection. This increase in temperature is due to activation of the thermoregulatory centre in the hypothalamus in response to exogenous and endogenous pyrogens [10]. Exogenous pyrogens include viruses, bacteria, allergens or immune complexes, while endogenous pyrogens include cytokines (interleukin 1 and 6) and tumour necrosis factor, released by stimulated monocytes and macrophages. During the reaction, there is increased expression of hypothalamic cyclooxygenase 2 (COX-2) and production of prostaglandin E2 (PGE2). The thermoregulatory centre is activated and switched to a higher thermal equilibrium point [33]. A number of changes, such as constriction or dilation of blood vessels, occur to achieve a higher body temperature, resulting in a decrease or increase in temperature in a particular area of the body. The circulation of body fluids in the dental organ is of great importance in the process of maintaining the homeostasis of the dental pulp and the nerves and odontoblasts contained within it [45], [46]. The lymphatic system provides an alternative means of recirculating intercellular fluid, while also becoming a defence against potential bacterial infection associated with pathological processes in the oral cavity. Understanding the mechanisms of angiogenesis and lymphangiogenesis during these processes may be beneficial for

more effective disease management, but further research is needed.

Lymphoscintigraphy is currently the gold standard for imaging lymphatic vessels. It is a well-established nuclear medicine technique for assessing lymphatic function by obtaining images of the lymphatic system using gamma rays after injection of small amounts of radiotracers [14], [36]. This technique is mainly used to differentiate lymphoedema from other causes of swelling and to delineate collateral lymphatics, the degree of vascular obstruction and the presence of abnormal lymphatic vessel collections [27].

The metabolic process is a fundamental aspect of human physiology, and its regulation is influenced by a multitude of factors. Illness, pregnancy and physical activity, for instance, can significantly alter metabolic rates when compared to a rested body in normal conditions. It is also noteworthy that the development of a disorder, such as local inflammation, can result in a local increase in metabolism.

In pathologically affected teeth, vasodilatation is observed in the pulp, accompanied by a variety of infiltrates [15]. These infiltrates are macrophage-lymphocytic or neutrophilic in nature. The nature of the infiltration is central to the nature of the lesions occurring in the teeth. According to some authors [21], [28], [35], neoangiogenesis occurs as a result of the ongoing inflammatory process, accompanied by the appearance of new – both blood and lymphatic – vessels. As a result, the flow of interstitial fluids in pathologically affected teeth is different from that in healthy teeth. Caries is one of many dental diseases accompanied by such phenomena. The aim of the study was to identify the difference in the rate of heat dissipation by vessels present in the dental pulp.

2. Materials and methods

For the subtraction thermography surveys, healthy and teeth affected by caries right after extraction were cut in the transverse axis on a diamond saw, dried thoroughly and immediately subjected to thermographic testing after being placed in saline.

Cut tooth samples were heated with a 250 W IR lamp from a distance of 12 cm to 40 ± 0.5 °C. There was no other heat sources in the room that could affect the sample from the heat emitter in the form of the lamp used for heating.

The recording of a sequence of thermograms during free cooling of the samples for 120 seconds was performed using a high-resolution thermal imaging camera FLIR P640 with a spacer ring enabling recording from a distance of approx. 3 cm. The results of subsequent thermograms were subtracted from the so-called zero thermogram, i.e., the thermogram taken at the beginning of the cooling process. Then, areas showing asymmetry in the temperature distribution were located. For three areas (ROI), temperature gradient graphs were created and for each sample, the values of dimensionless temperature indices were calculated. The obtained indices were compared with the so-called "gold standard", i.e., the result of lymphoscintigraphy. The sensitivity and specificity of the thermographic technique were assessed based on the analysis of ROC curves (determination of the cut-off value for each indicator).

Sequences of recorded thermograms were subjected to computer analysis using digital image analysis. A specialist software for thermogram analysis was used – ThermaCAM Researcher Pro 2.8 (FLIR Systems). The first step of the data analysis was to subtract the image after heating the samples with a lamp from the images recorded at different time points during free cooling at ambient temperature (T_{amb} = 22 ± 0.5 °C). The subtraction procedure enabled changes caused by sample heterogeneity to be more visible.

The thermal imaging survey was carried out in the following stages:

- Experimental determination of the temperature dependence of the tooth surface on its cooling time after heating with a long (up to 5 min.) thermal pulse of T_0 = 45 ± 0.5 °C;
- Performing *in vitro* tests on teeth with caries foci of various sizes, consisting of determining the dependence of the temperature distribution of the cross-sectional surface of the tooth (measurement temperature) on the cooling time at ambient temperature (T_{amb} = 22 ± 0.5 °C) stimulated by a thermal pulse;
- Calculation of the standard temperature contrast of the cross-sectional surfaces of the test teeth and determination of the dependence of the standard temperature contrast for individual tooth regions;
- Verification of the thermal imaging results obtained with the gold standard, which is the assessment using isotopes in lymphoscintigraphy and with X-ray examination.

Changes in the density of the tooth structure caused by the presence of the lymphatic system can be seen on the thermal imaging camera as differences in the rate of cooling or heating of different cross-sectional areas of the same tooth. Presumably regions with a high density of lymphatic vessels will be more porous, i.e.,

less dense, and thus slower to change their temperature during cooling.

Subtraction, a technique of subtracting thermograms taken at different times during the cooling process, was used with the aim of becoming independent of the emissivity coefficient values in different regions of the tooth cross–section. The subtraction operation of the two thermograms consisted of calculating for each pixel (1).

$$\boldsymbol{C}(i,j) = \text{Standarization}\left[\boldsymbol{A}(i,j) - \boldsymbol{B}(i,j)\right], \quad (1)$$

where the output images are denoted by ***A*** and ***B***, and the resultant image by ***C***.

Image ***A*** is the first thermogram recorded after the termination of the thermal effect (t = 0 s), while image ***B*** is one of a sequence of thermograms taken at successive seconds of cooling (after 60 s, 90 s and 120 s).

Subtraction operations were performed on isolated sections of the thermograms – ROI (*region of interest*), which contained only the part of the tooth that was of interest due to the presence of a defect (density of lymphatic vessels).

The thermographic test was carried out during the cooling process. Changes in the temperature distribution of a tooth previously heated to T_0 = 40 ± 0.5 °C during free cooling at ambient temperature 22 ± 0.5 °C were recorded. Two series of cooling measurements were performed for all teeth to enable validation of the proposed method (repeatability). All analyses of the thermogram sequences were carried out using ThermaCAM Researcher Pro 2.8 and MatLab (MathWorks) softwares. The temperature distribution of each tooth was measured twice, at intervals not exceeding 7 days. It made an analysis of the repeatability of the thermal imaging results (inter-rater reability possibly).

Due to the different surface condition of the cross-sectional area of the teeth examined (colour, roughness) and the associated different emissivity of the radiation, the changes in temperature (ΔT) of the tooth surface 120 s after turning off the thermal pulse (heating) were analyzed. After subtraction of the matrices of distribution of temperatures (in MatLab) taken at t = 0 s (matrix ***A***) and t = 120 s (matrix ***B***), matrix ***C*** was obtained to illustrate the changes in temperature of the tooth cross-sectional area that occurred after 2 min of convective cooling at ambient temperature (T_{amb} = 22 ± 0.5 °C).

The thermographic survey was carried out at the Faculty of Mechanical Engineering, Wrocław University of Science and Technology.

In the subtraction thermography study for selected tooth areas (ROI), basic descriptive statistics were estimated: means (M), standard deviations (±SD), minimum (Min) and maximum (Max) values, and temperature distribution symmetry indices. A non-linear regression analysis was used for building mathematical models of temperature change over time. The Bland–Altman method was used for assessing the repeatability of the measurement results and the correlation coefficient between the result of the first and second measurements was calculated. Calculations were performed using Statistica v.13 (TIBCO, Software Inc., USA). Temperature indices were calculated for each sequence of thermograms (samples).

3. Results

Directly recorded example thermograms are shown in Fig. 1.

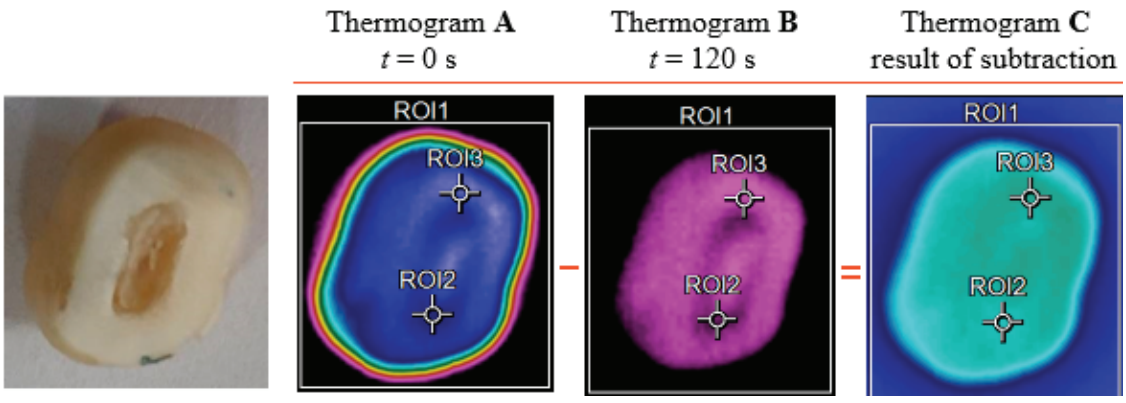

Fig. 1. Photograph of the cross-sectional surface of tooth no. 13 and thermograms with marked regions (ROI):
ROI1 – maximum temperature of the ROI1 region (tooth cross-section contour),
ROI2 – region with the smallest temperature difference (potential site for the presence of vessels),
ROI3 – region of greatest temperature difference – homogeneous structure (no gaps in tissues).
The concept of subtraction of thermograms: ***A*** − ***B*** = ***C***

3.1. Temperature indices

Indices for the cross-sections teeth should correlate with the status of the teeth (caries severity and vascular density). In contrast, in Figure 2, an example of the temperature drop in ROI2 (ΔT_{ROI2}) and ROI3 (ΔT_{ROI3}) regions of tooth no. 12 during free cooling and mathematical models is shown.

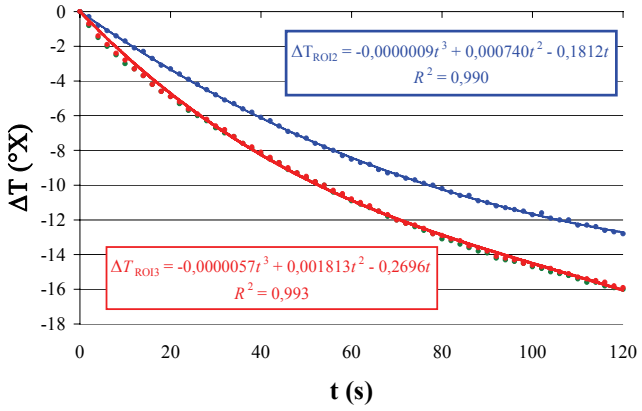

Fig. 2. Example of temperature drop in ROI2 (ΔT_{ROI2}) and ROI3 (ΔT_{ROI3}) regions of tooth no. 12 during free cooling and mathematical models

A sequence of thermograms of the cross-sectional surfaces of the test teeth was recorded at 30 Hz for 120 s of the free cooling process. Due to the low dynamics of temperature changes, only 12 thermograms recorded at 2 s intervals were used for statistical analysis. The shape of the cooling curves of the analyzed regions of the tooth's cross-sectional area depends, among other things, on the size of the vascular bed (but also on the severity of carious lesions).

In Table 2, the results of measuring the lowest temperature in two regions is shown, the location of which was determined by analyzing the resulting ***C*** thermogram, which is the difference in temperature distributions at the time the thermal excitation was switched off (t = 0 s) and after 120 seconds. The ROI3 region corresponds to the site on the tooth surface with the largest temperature difference and the ROI2 region to the smallest (Fig. 3). The ROI1 region covered the entire area of the chewing surface of the tooth.

In Figure 3 illustrates example temperature distributions on the surface of tooth no. 12 at the beginning (t = 0 s, figure **A**) and end of the cooling process (t = 120 s, figure **B**) from an initial temperature of T_0 = 40.5 °C to a final temperature of T_{120} = 24.5 °C. In this way, the influence of different emissivity coefficient values in different regions of the tooth surface was eliminated. On this basis, two areas of 3 × 3 pixels with the largest (ROI3) and smallest (ROI2) temperature differences were determined on the thermograms. Also, using a polygon, a rectangle (ROI1) describing the test tooth surface was determined.

- ROI1 – a rectangle circumscribed around the tooth cross-section contour marked in green;
- ROI2 – the area of the tooth surface with the largest vascular bed (smallest temperature change), shown in blue in protocols;
- ROI3 – the area with the smallest vascular bed (fastest temperature change), shown in red in protocols.

The recording time of the transient (cooling) process was set at 120 s and the sampling frequency at 1 Hz (sufficient due to the low dynamics of the cooling process). Each sequence (measurement) comprised 120 thermograms, which were then analyzed using ThermaCAM Researcher Pro 2.8 (FLIR Systems). The minimum temperature (T_{min}), maximum temperature (T_{max}), mean (T_{mean}) and standard deviation (SD_T) were read from each analyzed thermogram (ROI) region. Mean values (T_{mean}) were used for plotting the cooling curves.

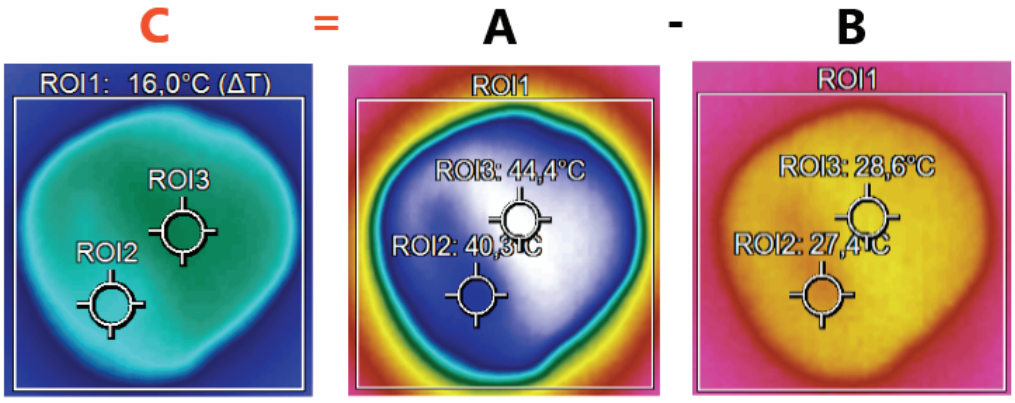

Fig. 3. Distribution of the temperature difference in the cross-sectional surface of tooth no. 12 after 120 s of cooling with the following marked regions: ROI2 – lowest temperature difference, ROI3 – highest difference

3.2. Temperature contrast

Based on the results of the measurements of temperature changes in the ROI2 and ROI3 regions, the so-called temperature contrasts – $C(t)$ were determined from the dependence (2).

$$C(t=60)=\frac{\Delta T_{\mathrm{ROI3}}(t=60)-\Delta T_{\mathrm{ROI3}}(t=0)}{\Delta T_{\mathrm{ROI3}}(t=60)-\Delta T_{\mathrm{ROI2}}(t=0)} \quad (2)$$

For example, the temperature contrasts at 30, 60 and 120 seconds of cooling were calculated for the data in Table 1, as (3)–(5).

$$C(t=30)=\frac{-1.8-0.0}{-1.4-0.0}=1.455\,, \quad (3)$$

$$C(t=60)=\frac{-1.3-0.0}{-1.1-0.0}=1.309\,, \quad (4)$$

$$C(t=120)=\frac{-0.8-0.0}{-1.0-0.0}=1.225\,. \quad (5)$$

and a summary index $C(t)$ which is the geometric mean of 12 contrasts:

$$C(t)=\sqrt[12]{C(t=10)\cdot C(t=20)\cdot\ldots\cdot C(t=180)}=1.370\,. \quad (6)$$

The temperature contrast showed distinct areas with different cooling rates.

Table 1. Example results of temperature measurement and temperature variation of tooth no. 12

t [s]	i	Temperature in tooth regions				$C(t)$
		T_{ROI2}	T_{ROI3}	ΔT_{ROI2}	ΔT_{ROI3}	
0	–	40.3	44.4	0.0	0.0	–
10	1	39.0	41.8	−1.3	−2.6	2.000
20	2	37.3	39.8	−1.7	−2.0	1.533
30	3	35.9	38.0	−1.4	−1.8	1.455
40	4	34.6	36.6	−1.3	−1.4	1.368
50	5	33.3	35.1	−1.3	−1.5	1.329
60	6	32.2	33.8	−1.1	−1.3	1.309
70	7	31.3	32.8	−0.9	−1.0	1.289
80	8	30.4	31.8	−0.9	−1.0	1.273
90	9	29.7	30.9	−0.7	−0.9	1.274
100	10	29.1	30.1	−0.6	−0.8	1.277
110	11	28.4	29.4	−0.7	−0.7	1.261
120	12	27.4	28.6	−1.0	−0.8	1.225
Mean						1.370

t – time (s), i – temperature measurement result number, T_{ROI2} – temperature at point ROI2, T_{ROI3} – temperature at point ROI_3, ΔT_{ROI2} – temperature change at point ROI_2, Δ_{ROI3} – temperature change at point ROI_3, $C(t)$ – temperature contrasts.

Staining scale of: 0–2, where 0 – no reaction, 1 – weak reaction, 2 – strong reaction.

3.3. Rate of temperature changes

Another way to describe the temperature change during cooling is to determine the so-called rate of change (decrease) in the average temperature of the region, determined from measurements taken as a time series with a fixed interval (Δt = 10 s). The rate change of G was calculated as the geometric mean of the variable-base indices calculated from the dependence (7).

$$i_{(i)}=\frac{T(i-1)}{T(i)}\cdot 100\,, \quad (7)$$

where: i = 1, 2, 3, ..., 12 – numbers of temperature measurements after 10, 20, 30, ..., 120 seconds. An example calculation for tooth no. 12 is shown in Table 2.

Table 2. Temperature measurement and rate of change indexes for tooth no. 12

t (s)	i	Temperatures in tooth regions		Indexes	
		T_{ROI2}	T_{ROI3}	i_{ROI2}	i_{ROI3}
0	–	40.3	44.4	–	–
10	1	39.0	41.8	96.77	94.14
20	2	37.3	39.8	95.64	95.22
30	3	35.9	38.0	96.25	95.48
40	4	34.6	36.6	96.38	96.32
50	5	33.3	35.1	96.24	95.90
60	6	32.2	33.8	96.70	96.30
70	7	31.3	32.8	97.20	97.04
80	8	30.4	31.8	97.12	96.95
90	9	29.7	30.9	97.70	97.17
100	10	29.1	30.1	97.98	97.41
110	11	28.4	29.4	97.59	97.67
120	12	27.4	28.6	96.48	97.28

t – time (s), i – temperature measurement result number, T_{ROI2} – temperature at point ROI2, T_{ROI3} – temperature at point ROI_3, i_{ROI2} – temperature rate of change index at point ROI2, i_{ROI3} – temperature rate of change index at point ROI3.

4. Discussion

Thermography is used in various fields of science and medicine – from sports medicine, dentistry, oncology to industry and construction. However, in the case of training, we can observe the response of the tissue stimulated in the results of exercise. The temperature map then shows distinct changes depending on how long the body cools down after the stimulus [24], [44].

Metabolic processes are considered to be the primary source of thermal energy in the body. According to

the available literature, nearly 60% of total energy is utilized for the generation of heat. Analysis of the temperature distribution on the surface allows to study inflammation, infection, tissue damage, connective tissue damage and the degree of congestion in organs throughout the body [35]. This is based upon the fact, that hyperaemic tissuses are able to transport more free energy in form of heat. This is associated with increased production by tissues or this is an element of thermoregulation, where dilated vessels help in heat release to the outside of the body [26].

Therefore, thermography is further used in the study of thermoregulation, detection of breast cancer, diagnostics of diabetic neuropathy and vascular disorders, measurement of body temperature, dental diagnostics, dermatology, blood pressure monitoring, diagnostics of rheumatic diseases, diagnostics of dry eye syndrome and eye diseases, diagnostics of liver diseases, kidney treatment, heart surgeries, gynaecology, personality testing and brain imaging [28], [32], [40].

The measurement of temperature as a diagnostic procedure with human teeth has been described with the use of thermocouples, infrared thermometers, miniature thermometers, thermistors, infrared thermography and cholesterol liquid crystals [21], [30], [43].

In 1996, Gratt et al. developed a new classification system using thermograms for patients with chronic orofacial pain. Thermograms were classified as normal, hot and cold when the selected ΔT values of the anatomical area (temperature difference on the right and left side) were 0–0.25 °C – above 0.35 °C and below 0.35 °C, respectively. Gratt et al. [16] reported that hot thermograms give a clinical diagnosis of sympathetic pain, peripheral nerve-mediated pain, temporomandibular joint (TMJ) arthropathy or sinusitis, while cold thermograms give a clinical diagnosis of peripheral nerve-mediated pain or pain independent of the sympathetic nervous system [4], [16], [17].

Normal thermograms included those with a clinical diagnosis of cracked tooth syndrome, trigeminal neuralgia, pretrigeminal neuralgia or psychogenic facial pain. This methodology proved to be accurate in 92% of cases. Asymptomatic TMJ patients were shown to have symmetrical thermal patterns with mean ΔT values of 0.1 °C, whereas TMJ pain patients showed asymmetrical thermal patterns with increased temperature over the affected TMJ area with mean ΔT values of 0.4 °C [28].

Canavan et al. [4] studied a group of patients with mild to moderate temporomandibular joint dysfunctions (TMDs) and found that ΔT values were correlated with patients' pain levels. Gratt et al. report that IRT of the chin is an effective method for diagnosing inferior alveolar nerve (IAN) deficits.

Despite its many advantages, electrothermal detachment (ETD) that is a common orthodontic bracket detachment method can cause thermal damage to the dental pulp. Cummings et al. [9] conducted in vitro studies using IRT on extracted human premolar teeth and found that during ETD, pulp temperature increases from 16.8 to 45.6 °C, causing severe pulp tissue damage.

Smith et al. [42] stated that change in the surface temperature of teeth is not suitable as a simple clinical means to assess pulp vitality. However, others found that teeth with non vital pulp have lower temperatures than teeth with vital pulp.

Many dental conditions are associated with disturbances in nerve conduction and blood flow [49]. Lahiri et al. [28] were able to directly demonstrate the relationship of vascular bed size to heat transfer rate.

Thermography can be used as a screening method for conditions in various dental specialties. Changes in the pattern of normality can be an indicator of pathological conditions [18], [20], [31].

Thermography is also used in orthodontics during the cementation of orthodontic brackets. The temperature rise of the composite material on which the orthodontic brackets are cemented must be controlled to prevent overheating of the dental pulp [2].

In endodontics, the most common reason for root canal treatment is pulpitis, which causes pain to the patient. The absolute temperature limit for restorative procedures in a dental organ is 41.5 °C. Above this temperature, pulpitis and even necrosis may occur [1]. Caries present within the dental pulp connects to the dental pulp via the dentinal tubules. Monitoring intertubular temperature through the use of thermography may help to identify and differentiate inflammatory conditions such as acute pulpitis with apical periodontitis (endo-perio lesions) 36 ± 0.5 °C, acute periapical abscess 37 ± 0.4 °C and chronic periapical abscess 35 ± 0.6 °C [1], [22], [33].

Thermography is also used for detecting changes in tooth decay (caries) at an early stage. A temperature of 49.66 °C suggests the presence of decalcification of the tooth enamel. Thermography may help in its identification of caries in areas that are visually difficult to access clinically, complementing radiographic imaging in the diagnostics of carious lesions [44]. The use of thermal imaging in orthodontics makes it possible to monitor, among other things, the variation in tooth temperature rise during electrothermal removal of orthodontic brackets, avoiding the high risk of overheating of the dental pulp. It also makes it pos-

sible to analyze cross-sections of teeth during the process of removing ceramic brackets using a CO_2 laser [2].

In the field of surgery, thermography is very useful for quantifying the cutaneous inflammatory response after surgical removal of retained teeth [7], [23]. Some studies identified changes in the facial circulatory system after extraction of third molars and found that regional blood flow might change after surgical trauma and increase local circulation. This happens mainly in the lymphatic microcirculation. This biological process may cause a temporary local rise in temperature [3]. In orthognathic surgery, thermography quantifies facial temperature in patients undergoing maxillary and mandibular osteotomy [13].

In our study, subtractive thermography was used to detect areas of different energy dissipation time, indicating different density and heat conduction capacity of the teeth. This indicates the heterogeneity of the tooth structure resulting from damage to the wall by the developing carious process. the accompanying inflammation also leads to the expansion of vessels, which are capable of bringing more energy from the teeth. This release proved to be useful in assessing the presence of a vascular bed in the dental pulp under physiological and pathological conditions.

The limitations of the study include the low number of teeth analyzed in both groups. Furthermore, the inability to distinguish between lymphatic and blood vessels on examination.

5. Conclusions

Hyperaemia as a result of inflammation is associated with increased blood flow, thus, an increased temperature of a tooth. Thermography can detect these temperature changes so high resolution thermography may be used for diagnostic purposes. The active dynamic thermography confirmed the presence of areas of various sizes, which indicate the changes in fluids drainage and, consequently, heat. This is indicative of the inflammation-induced change in the size of the bed that allows the circulation of body fluids – blood and lymph.

Acknowledgements

The review article is part of SUB.B080.21.075 and STM. B080.17.059 research projects of the Wroclaw Medical University, Wrocław, Poland.

References

[1] ABOUSHADY M.A., TALAAT W., HAMDOON Z., M ELSHAZLY T., RAGY N., BOURAUEL C., TALAAT S., *Thermography as a non-ionizing quantitative tool for diagnosing periapical inflammatory lesions*, BMC Oral Health. 2021, May 13, 21 (1), 260.

[2] AKSAKALLI S., DEMIR A., SELEK M., TASDEMIR S., *Temperature increase during orthodontic bonding with different curing units using an infrared camera*, Acta Odontol. Scand., 2014, 72 (1), 36–41.

[3] BAGAVATHIAPPAN S., SARAVANAN T., PHILIP J., JAYAKUMAR T., RAJ B., KARUNANITHI R., MR PANICKER T., KORATH P., JAGADEESAN K., *Investigation of peripheral vascular disorders using thermal imaging*, Br. J. Diabetes Vasc. Dis., 2008, 8 (2), 102–104.

[4] CANAVAN D., GRATT B.M., *Electronic thermography for the assessment of mild and moderate temporomandibular joint dysfunction*, Oral Surg. Oral Med. Oral Pathol. Oral Radiol. Endod., 1995, 79 (6), 778–786.

[5] CHÁVEZ DE PAZ L.E., BERGENHOLTZ G., SVENSÄTER G., *The effects of antimicrobials on endodontic biofilm bacteria*, J. Endod., 2010, 36 (1), 70–77.

[6] CHÁVEZ DE PAZ L.E., ZAPATA R.O., *Challenges for root canal irrigation: microbial biofilms and root canal anatomy*, Endo. Ept., 2019, 91–100.

[7] CHRISTENSEN J., MATZEN L.H., VAETH M., SCHOU S., WENZEL A., *Thermography as a quantitative imaging method for assessing postoperative inflammation*, Dentomaxillofac Radiol., 2012, 41 (6), 494–499.

[8] COUVE E., OSORIO R., SCHMACHTENBERG O., *The amazing odontoblast: activity, autophagy, and aging*, J. Dent. Res., 2013, 92 (9), 765–772.

[9] CUMMINGS M., BIAGIONI P., LAMEY P.J., BURDEN D.J., *Thermal image analysis of electrothermal debonding of ceramic brackets: an in vitro study*, Eur. J. Orthod., 1999, 21 (2), 111–118.

[10] DINARELLO C.A., *Infection, fever, and exogenous and endogenous pyrogens: some concepts have changed*, J. Endotoxin. Res., 2004, 10 (4), 201–222.

[11] DURAND S.H., FLACHER V., ROMÉAS A., CARROUEL F., COLOMB E., VINCENT C., MAGLOIRE H., COUBLE M.L., BLEICHER F., STAQUET M.J., LEBECQUE S., FARGES J.C., *Lipoteichoic acid increases TLR and functional chemokine expression while reducing dentin formation in in vitro differentiated human odontoblasts*, J. Immunol., 2006, 1, 176 (5), 2880–2887.

[12] EL-KEBIR H., RAN J., LEE Y., CHAMORRO L.P., OSTOJA-STARZEWSKI M., BERLIN R., AGUILUZ CORNEJO G.M., BENEDETTI E., GIULIANOTTI P.C., BENTSMAN J., *Minimally Invasive Live Tissue High-fidelity Thermophysical Modeling using Real-time Thermography*, ArXiv., 2023, 23, arXiv: 2301.09733.

[13] ENDO T., KOMATSUZAKI A., MIYAGAWA Y., KAMODA T., GOTO S., KOIDE K., MIZUTANI M., *Thermographic assessment of facial temperature in patients undergoing orthognathic surgery*, J. Oral Sci., 2019, 61 (2), 321–326.

[14] FORTE A.J., BOCZAR D., HUAYLLANI M.T., LU X., CIUDAD P., *Lymphoscintigraphy for Evaluation of Lymphedema Treatment: A Systematic Review*, Cureus., 2019, 12, 11 (12), e6363.

[15] GALLER K.M., WEBER M., KORKMAZ Y., WIDBILLER M., FEUERER M., *Inflammatory Response Mechanisms of the Dentine-Pulp Complex and the Periapical Tissues*, Int. J. Mol. Sci., 2021, 2, 22 (3), 1480.

[16] GRATT B.M., GRAFF-RADFORD S.B., SHETTY V., SOLBERG W.K., SICKLES E.A., *A 6-year clinical assessment of electronic fa-*

cial thermography, Dentomaxillofac. Radiol., 1996, 25 (5), 247–255.

[17] GRATT B.M., SICKLES E.A., SHETTY V., *Thermography for the clinical assessment of inferior alveolar nerve deficit: a pilot study*, J. Orofac. Pain., 1994, 8 (4), 369–374.

[18] HADDAD D.S., BRIOSCHI M.L., ARITA E.S., *Thermographic and clinical correlation of myofascial trigger points in the masticatory muscles*, Dentomaxillofac. Radiol., 2012, 41 (8), 621–629.

[19] HAHN C.L., LIEWEHR F.R., *Update on the adaptive immune responses of the dental pulp*, J. Endod., 2007, 33 (7), 773–781.

[20] IOSIF L., MURARIU-MĂGUREANU C., PREOTEASA E., BĂRBÎNȚĂ--PĂTRAȘCU M.E., PREOTEASA C.T., *Infrared radiation in dentistry; measuring heat emission through passive method of thermography*, Rom. J. Phys., 2021, 66, 704, 1–15.

[21] JAFARZADEH H., UDOYE C.I., KINOSHITA J., *The application of tooth temperature measurement in endodontic diagnosis: a review*, J. Endod., 2008, 34 (12), 1435–1440.

[22] JAYARAJ A., JAYAKRISHNAN, SATISH S.V., NILLAN SHETTY K., RAI R., *Recent Advances in Endodontics Exploring the Trends in Diagnosis*, Int. J. Innov. Res. Sci. Eng. Technol., 2020, 5 (1), 219–222.

[23] KASPRZYK-KUCEWICZ T., CHOLEWKA A., BAŁAMUT K., KOWNACKI P., KASZUBA N., KASZUBA M., STANEK A., SIEROŃ K., STRANSKY J., PASZ A., MORAWIEC T., *The applications of infrared thermography in surgical removal of retained teeth effects assessment*, J. Therm. Anal. Calorim, 144, 2021, 139–144.

[24] KASPRZYK-KUCEWICZ T., SZURKO A., STANEK A., SIEROŃ K., MORAWIEC T., CHOLEWKA A., *Usefulness in Developing an Optimal Training Program and Distinguishing between Performance Levels of the Athlete's Body by Using of Thermal Imaging*, Int. J. Environ. Res. Public Health, 2020, 6, 17 (16), 5698.

[25] KASZUBA N., KASPRZYK-KUCEWICZ T., BAŁAMUT K., MORAWIEC T., STANEK A., WZIĄTEK-KUCZMIK D., CHOLEWKA A., *May thermal imaging be useful in the assessment of dental anaesthesia? Preliminary study*, J. Therm. Anal. Calorim, 2022, 147, 6745–6753.

[26] KOSIOR P., KLIMAS S., NIKODEM A., WOLICKA J., DIAKOWSKA D., WATRAS A., WIGLUSZ R.J., DOBRZYŃSKI M., *An in vitro examination of fluoride ions release from selected materials – resin-modified glass-ionomer cement (Vitremer) and nanohybrid composite material (Tetric EvoCeram)*, Acta Bioeng. Biomech., 2023, 25 (1), 101–115.

[27] KRAMER E.L., *Lymphoscintigraphy: defining a clinical role*, Lymphat. Res. Biol., 2004, 2 (1), 32–37.

[28] LAHIRI B.B., BAGAVATHIAPPAN S., JAYAKUMAR T., PHILIP J., *Medical applications of infrared thermography: A review*, Infrared Phys. Technol., 2012, 55 (4), 221–235.

[29] LARSEN T., *Susceptibility of Porphyromonas gingivalis in biofilms to amoxicillin, doxycycline and metronidazole*, Oral Microbiol. Immunol., 2002, 17 (5), 267–271.

[30] LAU X.E., LIU X., CHUA H., WANG W.J., DIAS M., CHOI J.J.E., *Heat generated during dental treatments affecting intrapulpal temperature: a review*, Clin. Oral Investig., 2023, 27 (5), 2277–2297.

[31] MENDES S., MENDES J., MOREIRA A., PAIS CLEMENTE M., VASCONCELOS M., *Thermographic assessment of vital and non-vital anterior teeth: A comparative study*, Infrared Phys. Technol., 2020, 106, 103232.

[32] NASUTION A.I., PANKOV M.N., *The Advantage and Basic Approach of Infrared Thermography in Dentistry*, J. Int. Dent. Med. Res., 2020, 13 (2), 731–737.

[33] PARK J.Y., PILLINGER M.H., ABRAMSON S.B., *Prostaglandin E2 synthesis and secretion: the role of PGE2 synthases*, Clin. Immunol., 2006, 119 (3), 229–240.

[34] PIATTELLI A., RUBINI C., FIORONI M., TRIPODI D., STROCCHI R., *Transforming growth factor-beta 1 (TGF-beta 1) expression in normal healthy pulps and in those with irreversible pulpitis*, Int. Endod. J., 2004, 37 (2), 114–119.

[35] RAMIREZ-GARCIA LUNA J.L., BARTLETT R., ARRIAGA--CABALLERO J.E., FRASER R.D.J., SAIKO G., *Infrared Thermography in Wound Care, Surgery, and Sports Medicine: A Review*, Front. Physiol., 2022, 3, 13, 838528.

[36] RANZENBERGER L.R., PAI R.B., *Lymphoscintigraphy*, In: StatPearls. StatPearls Publishing, Treasure Island (FL), 2023, PMID: 33085360.

[37] RICUCCI D., LOGHIN S., SIQUEIRA J.F. Jr., *Correlation between clinical and histologic pulp diagnoses*, J. Endod., 2014, 40 (12), 1932–1939.

[38] RING E.F., AMMER K., *Infrared thermal imaging in medicine*, Physiol. Meas., 2012, 33 (3), R33–46.

[39] SHIBA H., MOURI Y., KOMATSUZAWA H., OUHARA K., TAKEDA K., SUGAI M., KINANE D.F., KURIHARA H., *Macrophage inflammatory protein-3alpha and beta-defensin-2 stimulate dentin sialophosphoprotein gene expression in human pulp cells*, Biochem. Biophys. Res. Commun., 2003, 11, 306 (4), 867–871.

[40] SINGH D., SINGH A.K., *Role of image thermography in early breast cancer detection – Past, present and future*, Comput. Methods Programs Biomed., 2020, 183, 105074.

[41] SLOAN A.J., PERRY H., MATTHEWS J.B., SMITH A.J., *Transforming growth factor-beta isoform expression in mature human healthy and carious molar teeth*, Histochem. J., 2000, 32 (4), 247–252.

[42] SMITH E., DICKSON M., EVANS A.L., SMITH D., MURRAY C.A., *An evaluation of the use of tooth temperature to assess human pulp vitality*, Int. Endod. J., 2004, 37 (6), 374–380.

[43] SOORI A., KOWSARY F., KASRAEI S., *Experimental estimation of the emissivity of human enamel and dentin*, Infrared Phys. Technol., 2020, 106, 103234.

[44] STRABURZYŃSKA-LUPA A., KORMAN P., ŚLIWICKA E., KRYŚCIAK J., OGURKOWSKA M.B., *The use of thermal imaging for monitoring the training progress of professional male sweep rowers*, Sci. Rep., 2022, 3, 12 (1), 16507.

[45] SZTYLER K., PAJĄCZKOWSKA M., NOWICKA J., RUSAK A., CHODACZEK G., NIKODEM A., WIGLUSZ R.J., WATRAS A., DOBRZYŃSKI M., *Evaluation of the microbial, cytotoxic and physico-chemical properties of the stainless steel crowns used in pediatric dentistry*, Acta Bioeng. Biomech., 2022, 24 (4), 127–137.

[46] SZYMONOWICZ M., RUSAK A., PAJĄCZKOWSKA M., NOWICKA J., WIŚNIEWSKA K., ŻYWICKA B., RYBAK Z., DOBRZYŃSKI M., *Assessment of cytotoxic and antimicrobial activity of selected gingival haemostatic agents – in vitro study*, Acta Bioeng. Biomech., 2020, 22 (3), 185–198.

[47] TABATABAEI N., MANDELIS A., AMAECHI B.T., *Thermophotonic lock-in imaging of early demineralized and carious lesions in human teeth*, J. Biomed. Opt., 2011, 16 (7), 071402.

[48] YOSHIMURA A., LIEN E., INGALLS R.R., TUOMANEN E., DZIARSKI R., GOLENBOCK D., *Cutting edge: recognition of Gram-positive bacterial cell wall components by the innate immune system occurs via Toll-like receptor 2*, J. Immunol., 1999, 1, 163 (1), 1–5.

[49] ZHAN C., HUANG M., YANG X., HOU J., *Dental nerves: a neglected mediator of pulpitis*, Int. Endod. J., 2021, 54 (1), 85–989.